TSINGHUA SCIENCE AND TECHNOLOGY
ISSNll1007-0214 10/10 pp360–370
DOI: 10.26599/TST.2018.9010111
Volume 24, Number 3, June 2019

Asynchronous Brain-Computer Interface Shared Control of Robotic Grasping

Wenchang Zhang, Fuchun Sun*, Hang Wu, Chuanqi Tan, and Yuzhen Ma

Abstract: The control of a high Degree of Freedom (DoF) robot to grasp a target in three-dimensional space using Brain-Computer Interface (BCI) remains a very difficult problem to solve. Design of synchronous BCI requires the user perform the brain activity task all the time according to the predefined paradigm; such a process is boring and fatiguing. Furthermore, the strategy of switching between robotic auto-control and BCI control is not very reliable because the accuracy of Motor Imagery (MI) pattern recognition rarely reaches 100%. In this paper, an asynchronous BCI shared control method is proposed for the high DoF robotic grasping task. The proposed method combines BCI control and automatic robotic control to simultaneously consider the robotic vision feedback and revise the unreasonable control commands. The user can easily mentally control the system and is only required to intervene and send brain commands to the automatic control system at the appropriate time according to the experience of the user. Two experiments are designed to validate our method: one aims to illustrate the accuracy of MI pattern recognition of our asynchronous BCI system; the other is the online practical experiment that controls the robot to grasp a target while avoiding an obstacle using the asynchronous BCI shared control method that can improve the safety and robustness of our system.

Key words: asynchronous Brain-Computer Interface (BCI); shared control; motor imagery; robotic grasping

1 Introduction

An electroencephalogram (EEG)-based Brain-Computer Interface (BCI) system recording the brain potentials via electrodes placed on the scalp can rebuild the neuromuscular bypass through an external device. People with impaired motor cortical neural systems, such as stroke patients, benefit from the use of brain-actuated robots in everyday life for self-care or rehabilitation training[1]. Such people can control a robot arm and hand[2], wheelchairs[3], or prosthetic devices[4] by their minds to grasp daily necessities. In the BCI system, there are many paradigms during mental task such as steady state visual evoked potential and P300 known as evoked potentials, and Motor Imagery (MI) by Event-Related Desyncronization and Synchronization (ERD/ERS) spontaneous potentials. A well-performing BCI system can be a hybrid system that combines and collocates these paradigms efficiently. Among these paradigms, MI is the most frequently used one because of the natural spontaneous signals used for building a BCI. MI-based BCI detects the changes of mu (8–12 Hz) and beta (13–28 Hz) rhythms according to the ERD/ERS potentials. However, MI signal analysis is a very challenging task

• Wenchang Zhang, Fuchun Sun, and Chuanqi Tan are all with the Department of Computer Science and Technology, Tsinghua University, State Key Lab. of Intelligent Technology and Systems, Beijing 100084, China. E-mail: wzszwc@163.com; fcsun@mail.tsinghua.edu.cn; tcq15@mails.tsinghua.edu.cn.
• Wenchang Zhang and Hang Wu are with Institute of Medical Support Technology, Academy of Military Sciences, Wandong Road, Tianjin 300161, China. E-mail: wzszwc@163.com; 2008.wuhang@163.com.
• Yuzhen Ma is with Drugs Control of PAP, Beijing 102613, China. E-mail: mayuzhen52@126.com.
* To whom correspondence should be addressed.
Manuscript received: 2018-06-26; revised: 2018-06-28; accepted: 2018-07-04

to complete because of the low signal-to-noise ratio. The user is required to perform repeated training to improve the accuracy of the MI pattern recognition. Furthermore, the feature extraction algorithm in the frequency-bands, time, and spatial domains of the EEG signal is very important for solving this problem.

In recent years, an increasing number of researchers have been devoted to studying and designing the EEG-based BCI system for helping stroke patients to control the high degree of freedom robot arm to grasp objects in the 3D-scene using their minds. Meng et al.[5] proposed a novel method that decomposes the 3D-space into two sequential low-dimensional planes to improve the high accuracy of direction controls via EEG-based BCI. However, this step-by-step sequential control should be performed under the predesigned paradigm framework. Furthermore, two key problems were not taken into account. First, their system was predesigned, and the user should perform activities according to the specified tasks strictly. Second, the control direction might be incorrect because of EEG decoding error.

Usually, the BCI is divided into synchronous and asynchronous modes. Most of the early BCIs are synchronous because of the ease of design. These early BCIs have predefined time windows for MI signal pattern recognition. The user should complete the given mental activity that is designed in advance while being guided by a specific cue or trigger stimulus. However, this process may fatigue the user if the task requires too much time. Recently, development of an asynchronous BCI system that classifies the MI pattern in real-time without a predesigned cue stimulus has gained increasing attention because the user can perform the mental task at any desired time. The whole control task is easier and more comfortable for the user using the asynchronous BCI system compared to the synchronous BCI system. Mason and Birch[6] first proposed a Low-Frequency Asynchronous Switch Design (LF-ASD) to evaluate the performance of an EEG asynchronous device. Their method showed lower mean error rates than two other ASDs. Subsequently, Townsend et al.[7] applied Receiver Operating Characteristics (ROC) curves to adjust the upper and lower thresholds for the classification of the "resting periods" and the "mental periods". Borisoff et al.[8] designed a two-state brain switch prototype for self-paced control; however, the error rates of their prototype were still too high for real world use. Chae et al.[9] designed an asynchronous direct-control system of MI-based EEG for humanoid robot navigation. Lisi and Morimoto[10] proposed an asynchronous BCI and analyzed the EEG signal associated with gait speed changes. They evaluated the performance according to the logistic model probability output by means of the ROC and the respective Area Under the Curve (AUC). From the above, ROC curves were commonly applied to find the proper threshold for classification and estimate the performance of the asynchronous BCI.

For asynchronous BCI systems, a switch of the automatic and BCI control is often designed to change the control model. Geng et al.[11,12] presented a 3-class asynchronous BCI to control a simulated robot via a self-paced online BCI. They designed a switch to change the control models between Automatic Control (AC) and Subject Control (SC) modes. Although the switching method was efficient at that time, only one control mode can be used at a specific time. It is generally known that the accuracy of BCI pattern recognition algorithm cannot reach 100%. Thus, recently, the use of the shared control strategy[13] becomes a trend of development for asynchronous BCI systems. Su et al.[14] proposed a Dual Control Path (DCP) method to improve the throughput of asynchronous pipeline. Their DCP had two control paths that were combined to control one data path. Millan et al.[15] presented an asynchronous and non-invasive BMI for the continuous control of an intelligent wheelchair. They implemented shared control techniques between the BMI and the intelligent wheelchair to assist the subject in the driving task. The results showed that subjects could rapidly achieve a significant level of mental control, even if far from optimal, to drive an intelligent wheelchair. Liu et al.[16] applied the supervisory theory of fuzzy discrete event system to design a shared controller for wheelchair moving control. Sun et al.[17] proposed a new shared controller based on the Fused Fuzzy Petri Nets (FFPNs) for brain-actuated robot control to grasp an object while avoiding an obstacle. The experimental results showed that the proposed method significantly improves the performance and robustness of the robotic control.

In this paper, we propose an asynchronous MI-based BCI system and apply the shared control method for brain-actuated robot grasping control. In this asynchronous MI-based BCI system, two detectors are designed: one is called the Intention Detector (ID), which discriminates the "rest" and "MI" states and has a threshold that can be adjusted according to ROC curves;

the other is the Motor Imagery Direction Classifier (MIDC) that classifies the MI pattern (left, right, and forward) by Low-Rank Linear Dynamical Systems (LR-LDS) modeling. Next, a shared control method is applied for the user mental control and robot AC to achieve the grasping task. The results of the experiment prove that our methods have a good performance. The user can control the robot hand moving direction via mental activity in the automatic grasping control process whenever desired. The contributions of this paper are listed as follows:

(1) Our proposed asynchronous BCI system has many advantages, such as high classification accuracy, no requirement for a predesigned EEG paradigm task, and ease of robotic control transformation.

(2) The shared control method can combines AC and BCI command intelligently, and it is easy to design and realize the asynchronous BCI system control for robotic grasping.

(3) The asynchronous BCI system is very practical and effective for robotic grasping. The robot hand can automatically move to the target while avoiding the obstacle on the BCI shared control conditions.

This paper is organized as follows. Section 2 describes our proposed system pipeline. The asynchronous MI-based BCI system is illustrated in Section 3; the system performs data acquisition, preprocessing for EEG, feature extraction, and online EEG classification converting to control command. Section 4 shows the shared control strategy for robotic grasping. Section 5 describes the experiments performed and analysis of the experimental results. Section 6 presents our conclusion.

2 System Architecture

Figure 1 shows the pipeline of our proposed system. The system includes two sub-systems: the asynchronous BCI system and the shared control system. For the asynchronous BCI system, EEG signals are first pre-processed and analyzed. Next, three MI patterns (“left hand”, “right hand”, and “tongue”) are used to control three directions as “left”, “right”, and “forward”, respectively. The training dataset of EEG is built to find the common features of MI pattern offline. Next, a suitable classifier can be trained for the online analysis of MI-based EEG. In the actual control stage, the ID works all the time to find the existence of MI from the asynchronous BCI. When the user sends the

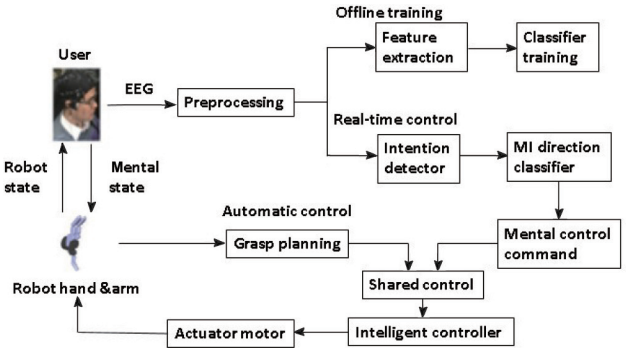

Fig. 1 Pipeline of the asynchronous BCI system.

MI signals, the classifier trained offline is applied to classify the MI pattern in a real-time window. The brain commands are translated to control the robotic grasping direction.

Moreover, the shared control system contains the mental control command system described above and the robot AC system that aims to plan the moving path for the robot hand and arm according to the vision feedback from Kinect. When the AC system starts to grasp an object, the user can mentally control the robotic hand moving direction at any time via the asynchronous BCI system. The user views the robot state and intervenes once the robotic planning path functions poorly. Therefore, the mental commands are detected by the asynchronous BCI in real-time. Next, the shared control method is applied to integrate these two control modes. Finally, the robot arm and hand can move via the actuator motor control to avoid the obstacle and reach the object.

3 Asynchronous MI Based BCI

3.1 Data acquisition

We apply a Neuroscan EEG-recording system with 32-channel electric potentials from the scalp of the user wearing an EEG cap to collect the EEG signals. The sampling frequency is 1000 Hz. The five healthy people within the age group of 20–28 years are selected as subjects.

The analysis of asynchronous BCI has two sessions: offline training and real-time control. The main purpose of offline training is feature extraction and classifier selection using machine learning algorithms. Figure 2 shows the offline training protocol. First, the rest periods last for 5 seconds, and each of the subjects keeps her/his brain idle to the best of her/his ability. After the rest period, each subject attempts to perform

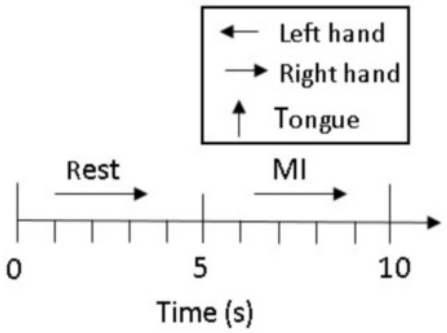

Fig. 2 Pipeline of the asynchronous BCI system.

the motor imagination task according to the three random MI cues displayed in the monitor. Ten trials are recorded from each subject, with 50 trials in total obtained. The BCI system processes the subject's ongoing EEG signal every 200 ms. The raw data of each trial can be represented by fifty 200×32 labeled matrices.

Next, the real-time control session detects the user's brain activity every 200 ms. Finishing feature extraction and classification, the mental pattern can be recognized by the trained classifier. Through a conversion algorithm, the mental control command of moving direction is sent from the BCI to the robot arm and hand every 1 s.

3.2 Pre-processing of EEG

Before EEG signal analysis, the following preprocessing methods are employed.

(1) Channel selection. We chose 21 channels over the motor cortex (CP6, CP4, CP2, C6, C4, C2, FC6, FC4, FC2, CPZ, CZ, FCZ, CP1, CP3, CP5, C1, C3, C5, FC1, FC3, and FC5) that are related to MI.

(2) Filtering. A Butterworth filter is employed for filtering of the EEG signals within a specific frequency band between 8 and 30 Hz, which encompasses both the alpha rhythm (8–13 Hz) and the beta rhythm (14–30 Hz) related to MI.

(3) ICA decompositions. We apply the "fastica" algorithm (Hyvarinen[18]) to decompose different neural artifacts because of its efficient and fast performance.

3.3 Feature extraction and classification

There are two steps in the asynchronous MI-based BCI: one is the use of the ID to detect the "rest" and "MI" states; the other is the use of the MIDC to discriminate the MI patterns as "left", "right" or "forward" after detecting MI in the ID step.

During the ID step, the Linear Discriminant Analysis (LDA) algorithm is applied as the classifier to find a linear hyper-plane that can separate the two classes of the "rest" and "MI" states. The classification probabilities can be calculated using MATLAB running Algorithm 1.

To improve the classification accuracy, a threshold is employed to adjust the probabilities for classification based on the similarity between the test data and the MI states training data. However, the brain is usually very active. There may be many other intentions and noise when the user performs mental task. Aiming to detect the MI pattern, the ROC[19,20] and the respective AUC are used to find a suitable threshold that balances the True Positives (TPs) and False Positives (FPs). The two axes of the ROC curve consist of the True Positive Rate (TPR) and the False Positive Rate (FPR). The former is a measure of sensitivity, and the latter is a measure of selectivity. These rates are defined as follows:

$$\begin{aligned} \mathrm{TPR} &= \frac{n_{\mathrm{TP}}}{n_{\mathrm{TP}} + n_{\mathrm{FN}}}, \\ \mathrm{FPR} &= \frac{n_{\mathrm{FP}}}{n_{\mathrm{TN}} + n_{\mathrm{FP}}} \end{aligned} \tag{1}$$

where $n_{\mathrm{TP}}, n_{\mathrm{FN}}, n_{\mathrm{TN}}$, and n_{FP} are the numbers of TP, false negative, true negative, and FP results, respectively. Thus, we adopt an all-or-nothing approach[21], in which the whole trial is represented by the epoch with the highest output probability. A balanced point is considered as a threshold that results in a TPR value equal to 1. FPR and the threshold value for that point are used to redefine the LDA threshold. From each ROC curve, a threshold corresponding to the point of the ROC curve closest to the line $y = 1 - x$ is selected as an indication of equal balance between TPs and FPs. Figure 3 shows the online classification performance. There are three curves that denote three mental patterns: "left", "right", and "forward". For example, if TP is the true positive of "left", then FP is the false positive that includes the "right", "forward", and "rest". When the thresholds of "left", "right", and "forward" are resulted as 0.6, 0.62, and 0.64, we obtain

Algorithm 1 Classification probabilities calculation

$W = \mathrm{LDA}(X, Y)$;
% LDA is the linear discriminant analysis function. W is linear discriminant coefficients, X are training data, Y are test data.
$L = [\mathrm{ones}(m, 1)X] \cdot W'$;
% L is linear scores for training data. m is the numbers of training data and test data.
$p = \exp(L)./\mathrm{repmat}(\mathrm{sum}(\exp(L), 2), [1\ \ 2])$;
% p is class probabilities.

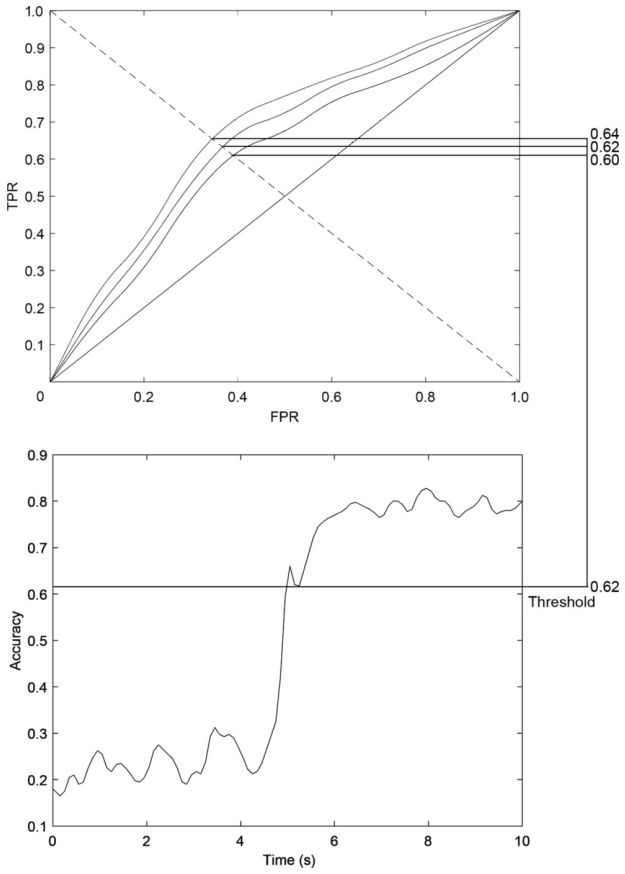

Fig. 3 Online classification performance. ROC curves determine the appropriate threshold values, and the average threshold discriminates the rest and MI time periods.

the final threshold of ID as the average value of 0.62. Therefore, the maximum accuracy of ID classifying the "rest" and MI states by LDA is approximately 80% when the threshold is 0.62.

Aiming to design the MIDC, Low-Rank Linear Dynamical Systems (LR-LDS) modeling[22] is applied for EEG signal feature extraction. The training EEG signal matrix $\boldsymbol{X}$ can be decomposed as

$$\boldsymbol{X} := \boldsymbol{A} + \boldsymbol{B} + \boldsymbol{E} \tag{2}$$

where $\boldsymbol{A} \in \mathbf{R}^{m\times n}$ is a low-rank matrix that contains the global information to describe the variant EEG signals, $\boldsymbol{B} \in \mathbf{R}^{m\times n}$ approximates invariant and denotes the same MI pattern, and $\boldsymbol{E} \in \mathbf{R}^{m\times n}$ is the matrix of sparse noise.

To calculate the matrices $\boldsymbol{A}, \boldsymbol{B}$, and $\boldsymbol{E}$, we add the orthogonal constraint and define the optimization problem formulation as

$$\min_{\boldsymbol{A},\boldsymbol{B},\boldsymbol{E}} \|\boldsymbol{A}\|_* + \alpha\|\boldsymbol{E}\|_1 + \beta\sum_{i\neq j}\|\boldsymbol{B}_i - \boldsymbol{B}_j\|_{\mathrm{F}}^2, \quad \text{s.t. } \boldsymbol{X} = \boldsymbol{A} + \boldsymbol{B} + \boldsymbol{E} \tag{3}$$

Next, the Augmented Lagrange Multiplier (ALM)[23] method is utilized to solve the above problem as follows:

$$L(\boldsymbol{A},\boldsymbol{B},\boldsymbol{E},\boldsymbol{\lambda}) = \|\boldsymbol{A}\|_* + \alpha\|\boldsymbol{E}\|_1 + \beta\sum_{i\neq j}\|\boldsymbol{B}_i - \boldsymbol{B}_j\|_{\mathrm{F}}^2 + \langle\boldsymbol{\lambda}, \boldsymbol{X} - \boldsymbol{A} - \boldsymbol{B} - \boldsymbol{E}\rangle + \frac{\mu}{2}\|\boldsymbol{X} - \boldsymbol{A} - \boldsymbol{B} - \boldsymbol{E}\|_{\mathrm{F}}^2 \tag{4}$$

where $\boldsymbol{\lambda}$ is a Lagrange multiplier matrix, and μ is a positive scalar.

Finally, the low-rank decomposition matrices $\boldsymbol{A}, \boldsymbol{B}$, and $\boldsymbol{E}$ are computed using MATLAB. We apply the EEGLAB toolbox developed by the Swartz Center for Computational Neuroscience to visualize the matrices, as plotted in Fig. 4.

Subsequently, we use the LDS algorithm[24] to extract the spatio-temporal feature matrix from $\boldsymbol{B}$ calculated above. Next, the Martin Distance[25, 26] is applied as the kernel to present distance of different LDS feature matrices. We can classify the EEG signals by comparing the Martin Distance between the training data and the testing data. The nearest two samples may be in the same class. Therefore, the forecast label and predict accuracy can be calculated using the k-Nearest Neighbor algorithm. Overall, our LR-LDS method finds the same invariant pattern of EEG effectively and extracts the spatio-temporal feature simultaneously. Thus, our LR-LDS method performs the MI pattern classification well.

3.4 Control command transformation

The dynamic fading feedback rule[20] is applied to determine the control commands. In our work, the classifications from the BCI are generated every 200 ms, and the direction commands control the robot hand to move for 1 s at a constant speed. Figure 5 illustrates an example for the control commands. For the first 2 s, the "rest" pattern appears every 0.2 s. When the classification result is same as the candidate decision, the selection level is increased by one level. Next, the "right" classifications increase gradually up to level 3. Thus, the asynchronous BCI generates a "right" control command for 1 s. The robot hand executes the motion and moves to the right direction accordingly. If the classification result is different that the candidate decision, then the selection level is decreased by one level. At 4.6 s, the classification "forward" reaches the level 3. Therefore, the asynchronous BCI generates a "forward" control command at that moment. The robot hand executes the motion and moves to the forward direction accordingly. Subsequently, the classification

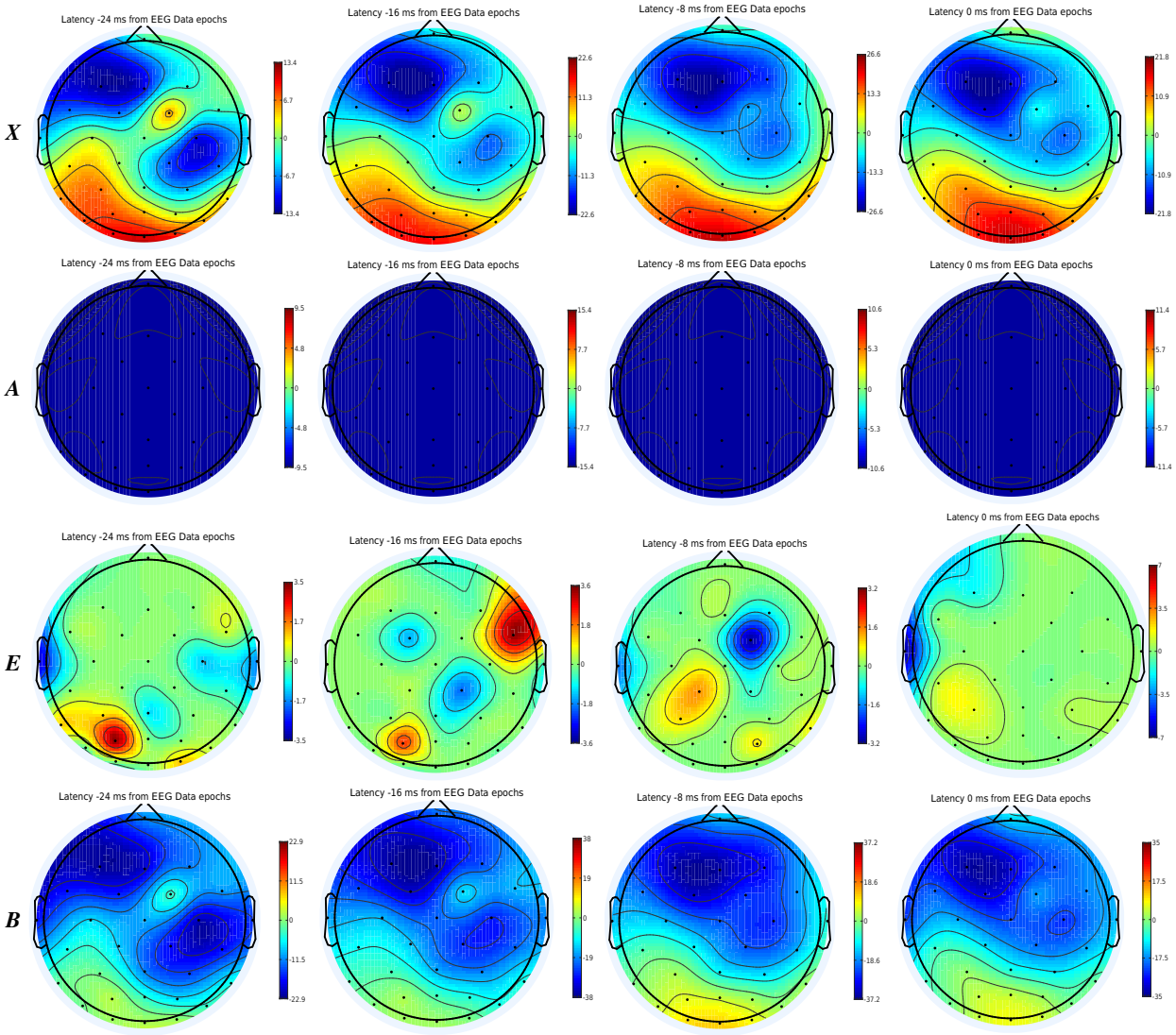

Fig. 4 Low-rank decomposition of EEG signal for the subject "right hand" MI at 0, 8, 16, and 24 ms (top to bottom: X, A, E, B). Note that A shows the global variant, E is the sparse noise, and B shares the same invariant pattern.

of BCI becomes the "idle" classification. There is no mental activity, so the robot still executes to moving command to grasp the object by automatic control.

4 Shared Control for Robotic Grasping

It is very difficult to achieve accurate control of high Degree of Freedom (DoF) robot arm through BCI step by step because it is almost impossible for the accuracy of MI pattern recognition to reach 100%. The shared control strategy for asynchronous BCI combines mental control by the MI EEG paradigm and AC based on robotic vision as feedback. Therefore, the shared control strategy has many advantages, such as no requirement for mental control all the time and improvement of the AC accuracy.

We applied the FFPNs method[17] to solve the shared control problem. The FFPN is defined as follows:

$$\text{FFPN} = (P, T, D, I, O, W, \Theta, f, \alpha, \beta) \qquad (5)$$

where P is a finite set of fuzzy places; T denotes a finite set of fuzzy transitions; D is a finite set of propositions; $I : P \times T \to \{0, 1\}$ is an input function that defines the set of directed arcs from P to T. O is an output function that defines the set of directed arcs from T to P; W is a weight function attached to the arcs (if this integer is missing, then it is assumed that the weight of the arc is 1); Θ denotes a mapping of the fuzzy transition to fuzzy transition subclass; f is an association function mapping from transitions to real values between zero and one. α is an association function mapping from places to real values between zero and one. β is an association

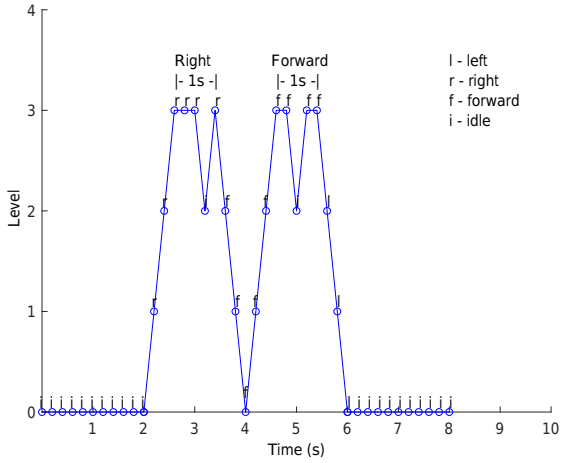

Fig. 5 Dynamic fading feedback rule for the variation of selection levels and classifications of a real-time BCI experiment over 8 s. The mental control commands every 0.2 s are transformed into the robotic control order every 1 s.

function, involving a bijective mapping from places to propositions. The Fuser transition function is defined as

$$F(x) = \sum x_i \times w_i, \quad \sum w_i = 1 \tag{6}$$

The FFPN for shared control fuses the moving direction of AC and the asynchronous BCI command. To control the high DoF robot arm to move to the object in 3D space, we should first reduce the dimension level to plane to ensure that the target and the robot hand are at the same height. The only control parameter is the moving direction of the robot hand originating from the AC and asynchronous BCI command in the same plane (Fig. 6).

The structure of FFPN for the shared control can be described as shown in Fig. 7.

P3 is calculated based on the fuzzy rule defining both W1 and W2. If the control command of BCI is not rational according to the robotic vision feedback, then W2 of BCI control should be set to a very small value (even to 0). If the BCI command is relatively rational, then the final direction can be calculated by the intelligent adjustment of W1 and W2, considering the distance from the robot hand to the obstacle.

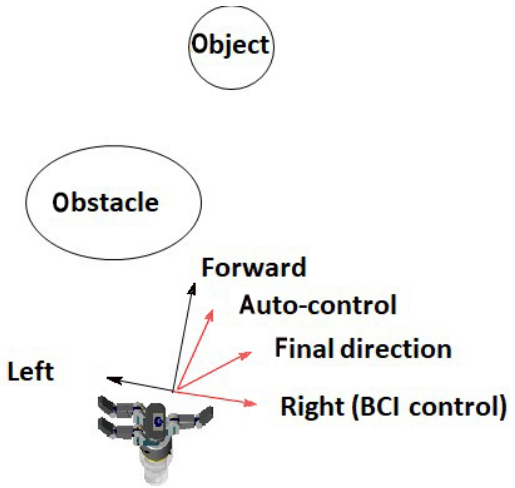

Fig. 6 Shared control of the robot hand moving direction.

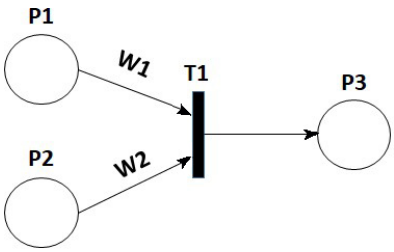

Fig. 7 FFPN for the shared control. P1 is a place that represents the AC of the moving direction. P2 is a place that denotes the asynchronous BCI control of the moving direction, including left, right, and forward. T1 is the fused fuzzy transition of shared control. P3 is the place of FFPN output representing the final moving direction. W1 and W2 are weights.

For example (Fig. 8), θ denotes the angle between the obstacle and the original moving direction and can be defined as fuzzy set (NB(–90°); NM(–60°); NS(–30°); Z(0°); PS(30°); PM(60°); PB(90°)), where N is negative; P is positive, B is big, M is middle, S is small. ω is the angle between the target and the AC direction and is calculated as PS based on the fuzzy rule. The distance from the robot hand to the obstacle is defined as N from the fuzzy set (N: near, M: middle, F: far). If the mental control direction is right, then it is rational based on the robotic vision and human experience. Therefore, the value of W2 should be increased. (W1, W2) can be set as (0.2, 0.8) according to the parameter adjustment. The value of α denoting the angle between the target and final output direction can be computer as

$$30° \times 0.2 + 90° \times 0.8 = 78°.$$

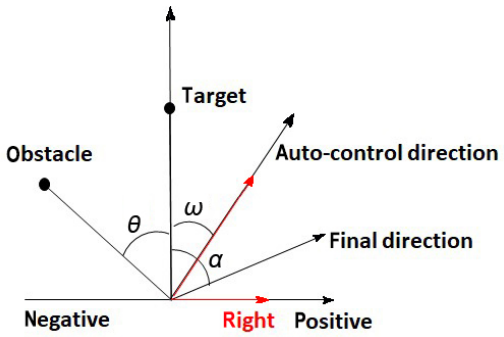

Fig. 8 FFPN calculation for the output of the moving direction.

5 Experiment

5.1 Asynchronous BCI system performance

The five subjects studied in the experiment manipulated the asynchronous MI based BCI system. The EEG signals were used to control the three directions (right, left, and forward) of the robot hand movement. The subjects rested or imaged right hand movement, left hand movement, and tongue movement according to the experiment procedure. Two steps were used: training paradigm and test paradigm. The aim of the training paradigm was to learn the different features of the subjects' EEG signals. We labeled the classifications of ten trails every 0.2 s from each subject during 5 s MI that was described in Section 3.1. To test the accuracy of our method, an additional four trials from each subject were recorded. Therefore, we obtained 100 labeled matrices to test the classification accuracy from each subject.

We performed a pair of contrast tests to illustrate the performance of our method. Test 1 applied Common Spatial Pattern (CSP)[27, 28] to extract the feature of EEG signals and used LDA to classify the MI patterns. Test 2 was our proposed method in this paper. The results of the two tests are listed as Table 1. We clearly observed that the accuracies of classification in Test 2 were all higher than those of Test 1. Our method with the threshold and the LR-LDS modeling method performed better.

5.2 Performance of grasping control

The experiment platform was based on the Barrett 3-finger hand, the SCHUNK 7-joint arm, and Kinect (Fig. 9). Our goal was to evaluate the contribution of our shared control for grasping an object.

In the applied shared control, the robot performed grasp planning intelligently using computer vision based on avoiding obstacle and achieving the shortest path planning all the time. The user asynchronously sent high-level commands via BCI whenever desired according to the experience of the user. The compared experiment aimed to illustrate the performance of shared control under two conditions: Asynchronous BCI with shared Control (AC) and Synchronous BCI Control (SC). We chose a bottle as the object for grasping. After the robot hand started to move, a cylinder box, serving as the obstacle, was randomly placed nearby the object. The experiments of each of the five subjects under AC and SC were conducted. Table 2 presents the results of the grasp success rate.

Table 1 Accuracy of classification by contrast tests. (%)

		Subject				
		a	b	c	d	e
Test 1	Right	63.6	60.6	69.7	66.7	54.5
	Left	66.7	63.6	63.6	63.6	57.6
	Up	58.8	61.8	67.6	55.9	55.9
	Average	63	62	67	62	56
Test 2	Right	72.7	69.7	81.8	72.7	75.8
	Left	69.7	75.8	75.8	78.8	72.7
	Up	70.6	64.7	73.5	58.9	70.6
	Average	71	70	77	70	73

Fig. 9 Experiment platform.

We found that there were four failures in the grasping task of SC because the robot arm faced interference from the obstacle. The primary cause of these failures is that the accuracies of EEG pattern classification were not 100%. The errors of classification led to the use of the wrong direction of robot arm movement to touch the obstacle. Our AC method could avoid the failure to the largest extent because the robot could amend the wrong control commands from asynchronous BCI according to the robotic vision feedback. Furthermore, the SC clearly cost much more time for moving the robot hand to the target, and the subjects should perform the MI paradigm task all the time, possibly resulting in fatigue of the brain. In contrast, the user could easily control the robot arm, using few MI interventions in the AC mode.

6 Conclusion

This paper presented a proposed asynchronous MI based BCI system for brain-actuated robotic grasping control. The proposed system allows the user to mentally control the moving direction of a robot hand and arm via BCI whenever the user feels it is necessary to adjust the moving path. To improve the accuracy of mental pattern classification, we designed the threshold and LDA classifier for the ID and used our LR-LDS modeling method for the MIDC in the system. In the proposed system, the dynamic fading feedback rule is

Table 2 Results of robotic grasping tasks. Five subjects (a, b, c, d, and e) controlled the robot arm to grasp object avoiding obstacle by BCI. ABC: asynchronous BCI with shared control; SBC: synchronous BCI control; n_{TP}: number of true positive events; n_{FP}: number of false positive events; n_{MN}: number of mental commands; ACC: accuracy of the MI classification; Min: task span; and Suc.: whether it was successful or not for the robotic grasping.

Subject	Method	Run	n_{TP}	n_{FP}	n_{MN}	ACC (%)	Min (s)	Suc.
a	ABC	1	10	5	3	66.7	23	Y
		2	13	7	4	65.0	28	Y
		3	11	4	3	73.3	24	Y
	SBC	1	86	39	25	68.8	130	Y
		2	55	25	16	68.9	86	N
		3	111	44	31	71.6	162	Y
b	ABC	1	18	7	5	72.0	32	Y
		2	10	5	3	66.7	22	Y
		3	11	4	3	73.3	26	Y
	SBC	1	101	39	28	72.1	142	Y
		2	85	35	24	70.8	126	Y
		3	71	29	20	71.0	108	N
c	ABC	1	8	2	2	80.0	21	Y
		2	7	3	2	70.0	23	Y
		3	11	4	3	73.3	25	Y
	SBC	1	100	45	29	70.0	152	Y
		2	116	44	32	72.5	168	Y
		3	97	38	27	71.9	138	Y
d	ABC	1	14	6	4	70.0	27	Y
		2	7	3	2	70.0	21	Y
		3	10	5	3	66.7	24	Y
	SBC	1	61	29	18	67.8	94	N
		2	86	44	26	66.2	133	Y
		3	43	17	12	71.7	70	N
e	ABC	1	11	4	3	73.3	23	Y
		2	15	5	4	75.0	27	Y
		3	9	6	3	60.0	24	Y
	SBC	1	81	39	24	67.5	125	Y
		2	101	44	29	70.0	150	Y
		3	107	38	27	73.8	142	Y

applied to convert the EEG classification results into control commands; next, the shared control approach combines the automatic grasping control of robot and mental control via our asynchronous MI-based BCI to grasp the object while avoiding an obstacle. The results of an experiment of MI classification illustrated that our method with the threshold and LDS modeling performs better than the classic CSP method. Furthermore, the practical experiment of the grasping task showed that our shared control method obtains higher success rate than the synchronous BCI control.

The use of the asynchronous BCI with shared control strategy is the trend for the brain-actuated robot development. Moreover, hybrid BCIs[29–34], which have the advantages of more analyzed commands for use to improve the overall performance of BCI system, have become a popular research topic in recent years. Therefore, an extension of our research involving application of the above methods can achieve real-time control of an advanced robot to perform more complex tasks via a comfortable and convenient BCI system.

Acknowledgment

This work was supported by the National Natural Science Foundation of China (Nos. 91420302 and 91520201) and Innovation Cultivating Fund Project $17-163-12-ZT-001-019-01$.

References

[1] J. N. Mak and J. R. Wolpaw, Clinical applications of brain-computer interfaces: Current state and future prospects, *IEEE Rev. Biomed. Eng.*, vol. 2, pp. 187–199, 2009.

[2] S. M. Grigorescu, T. Lüth, C. Fragkopoulos, M. Cyriacks, and A. Gräser, A BCI-controlled robotic assistant for quadriplegic people in domestic and professional life, *Robotica*, vol. 30, no. 3, pp. 419–431, 2012.

[3] F. Galán, M. Nuttin, E. Lew, P. W. Ferrez, G. Vanacker, J. Philips, and J. del R. Millán, A brain-actuated wheelchair: Asynchronous and non-invasive brain-computer interfaces for continuous control of robots, *Clin. Neurophysiol.*, vol. 119, no. 9, pp. 2159–2169, 2008.

[4] G. R. Muller-Putz and G. Pfurtscheller, Control of an electrical prosthesis with an SSVEP-based BCI, *IEEE Trans. Biomed. Eng.*, vol. 55, no. 1, pp. 361–364, 2008.

[5] J. J. Meng, S. Y. Zhang, A. Bekyo, J. Olsoe, B. Baxter, and B. He, Noninvasive electroencephalogram based control of a robotic arm for reach and grasp tasks, *Sci. Rep.*, vol. 6, p. 38565, 2016.

[6] S. G. Mason and G. E. Birch, A brain-controlled switch for asynchronous control applications, *IEEE Trans. Biomed. Eng.*, vol. 47, no. 10, pp. 1297–1307, 2000.

[7] G. Townsend, B. Graimann, and G. Pfurtscheller, Continuous EEG classification during motor imagery simulation of an asynchronous BCI, *IEEE Trans. Neural Syst. Rehabil. Eng.*, vol. 12, no. 2, pp. 258–265, 2004.

[8] J. F. Borisoff, S. G. Mason, and G. E. Birch, Brain interface research for asynchronous control applications, *IEEE Trans. Neural Syst. Rehabil. Eng.*, vol. 14, no. 2, pp. 160–164, 2006.

[9] Y. Chae, J. Jeong, and S. Jo, Toward brain-actuated humanoid robots: Asynchronous direct control using an EEG-based BCI, *IEEE Trans. Robot.*, vol. 28, no. 5, pp. 1131–1144, 2012.

[10] G. Lisi and J. Morimoto, EEG single-trial detection of gait speed changes during treadmill walk, *PLoS One*, vol. 10, no. 5, p. e0125479, 2015.

[11] T. Geng, J. Q. Gan, and H. S. Hu, A self-paced online BCI for mobile robot control, *Int. J. Adv. Mechatronic Syst.*, vol. 2, nos. 1/2, pp. 28–35, 2010.

[12] T. Geng and J. Q. Gan, Motor prediction in brain-computer interfaces for controlling mobile robots, in *Proc. 30th Annu. Int. Conf. IEEE Engineering in Medicine and Biology Society*, Vancouver, Canada, 2008, pp. 634–637.

[13] Q. Li, W. D. Chen, and J. C. Wang, Dynamic shared control for human-wheelchair cooperation, in *2011 IEEE Int. Conf. Robotics and Automation*, Shanghai, China, 2011, pp. 4278–4283.

[14] B. Su, L. Shen, L. Wang, Z. Y. Wang, Y. R. Wang, L. B. Huang, and W. Shi, DCP: Improving the throughput of asynchronous pipeline by dual control path. in *IEEE International Conference on High Performance Computing & Communications & IEEE International Conference on Embedded & Ubiquitous Computing*, 2014.

[15] J. del R. Millan, F. Galan, D. Vanhooydonck, E. Lew, J. Philips, and M. Nuttin, Asynchronous non-invasive brain-actuated control of an intelligent wheelchair, in *Proc. 2009 Annu. Int. Conf. IEEE Engineering in Medicine and Biology Society*, Minneapolis, MN, USA, 2009, pp. 3361–3364.

[16] R. Liu, Y. X. Wang, and L. Zhang, An FDES-based shared control method for asynchronous brain-actuated robot, *IEEE Trans. Cybernet.*, vol. 46, no. 6, pp. 1452–1462, 2016.

[17] F. C. Sun, W. C. Zhang, J. H. Chen, H. Wu, C. Q. Tan, and W. H. Su, Fused fuzzy petri nets: A shared control method for Brain Computer Interface systems, *IEEE Trans. Cognit. Dev. Syst.*, doi: 10.1109/TCDS.2018.2818173.

[18] A. Hyvarinen, Fast and robust fired point algorithms for independent component analysis, *IEEE Transactions on Neural Networks*, vol. 10, no. 3, pp. 626–634, 1999.

[19] G. Townsend, B. Graimann, and G. Pfurtscheller, Continuous EEG classification during motor imagery-simulation of an asynchronous BCI, *IEEE Trans. Neural Syst. Rehabil. Eng.*, vol. 12, no. 2, pp. 258–265, 2004.

[20] Y. Chae, J. Jeong, and S. Jo, Toward brain-actuated humanoid robots: Asynchronous direct control using an EEG-based BCI, *IEEE Trans. Robot.*, vol. 28, no. 5, pp. 1131–1144, 2012.

[21] A. Muralidharan, J. Chae, and D. M. Taylor, Extracting attempted hand movements from EEGs in people with complete hand paralysis following stroke, *Front. Neurosci.*, vol. 5, p. 39, 2011.

[22] W. C. Zhang, F. C. Sun, C. Q. Tan, and S. B. Liu, Low-rank linear dynamical systems for motor imagery EEG, *Comput. Intel. Neurosc.*, vol. 2016, p. 2637603, 2016.

[23] Z. C. Lin, M. M. Chen, and Y. Ma, The augmented Lagrange multiplier method for exact recovery of corrupted low-rank matrices, arXiv preprint arXiv: 1009.5055, 2010.

[24] W. C. Zhang, F. C. Sun, C. Q. Tan, and S. B. Liu, Linear dynamical systems modeling for EEG-based motor imagery brain-computer interface. in *Cognitive Systems and Signal Processing*, F. Sun, H. Liu, and D. Hu, eds. Springer, 2016, pp. 521–528.

[25] R. J. Martin, A metric for ARMA processes, *IEEE Trans. Signal Proc.*, vol. 48, no. 4, pp. 1164–1170, 2000.

[26] A. B. Chan and N. Vasconcelos, Classifying video with kernel dynamic textures, in *Proc. 2007 IEEE Conf. Computer Vision and Pattern Recognition*, Minneapolis, MN, USA, 2007, pp. 1–6.

[27] H. Ramoser, J. Muller-Gerking, and G. Pfurtscheller, Optimal spatial filtering of single trial EEG during imagined hand movement, *IEEE Trans. Rehab. Eng.*, vol. 8, no. 4, pp. 441–446, 2000.

[28] M. Grosse-Wentrup and M. Buss, Multiclass common spatial patterns and information theoretic feature extraction, *IEEE Trans. Biomed. Eng.*, vol. 55, no. 8, pp. 1991–2000, 2008.

[29] B. Z. Allison, Toward ubiquitous BCIs, in *Brain-Computer Interfaces*, B. Graimann, G. Pfurtscheller, and B. Allison, eds. Springer, 2009, pp. 357–387.

[30] Y. Q. Li, J. Y. Long, T. Y. Yu, Z. L. Yu, C. C. Wang, H. H. Zhang, and C. T. Guan, An EEG-based BCI system for 2-D cursor control by combining Mu/Beta rhythm and P300 potential, *IEEE Trans. Biomed. Eng.*, vol. 57, no. 10, pp. 2495–2505, 2010.

[31] P. Horki, T. Solis-Escalante, C. Neuper, and G. Müller-Putz, Combined motor imagery and SSVEP based BCI control of a 2 DoF artificial upper limb, *Med. Biol. Eng. Comput.*, vol. 49, no. 5, pp. 567–577, 2011.

[32] B. Z. Allison, C. Brunner, C. Altstätter, I. C. Wagner, S. Grissmann, and C. Neuper, A hybrid ERD/SSVEP BCI for continuous simultaneous two dimensional cursor control, *J. Neurosci. Methods*, vol. 209, no. 2, pp. 299–307, 2012.

[33] J. Y. Long, Y. Q. Li, H. T. Wang, T. Y. Yu, J. H. Pan, and F. Li, A hybrid brain computer interface to control the direction and speed of a simulated or real wheelchair, *IEEE Trans. Neural Syst. Rehabil. Eng.*, vol. 20, no. 5, pp. 720–729, 2012.

[34] E. W. Yin, Z. T. Zhou, J. Jiang, F. L. Chen, Y. D. Liu, and D. W. Hu, A novel hybrid BCI speller based on the incorporation of SSVEP into the P300 paradigm, *J. Neural Eng.*, vol. 10, no. 2, p. 026012, 2013.

Chuanqi Tan is a PhD candidate in Department of Computer Sciences and Technology of Tsinghua University. Before this, he was worked at baidu.com in 2014 and jike.com in 2012. He received the master's degree from Beijing University of Technology in 2012. His research interests include artificial intelligence, deep learning, transfer learning, and brain-computer interface.

Yuzhen Ma received the BS degree from Third Military Medical University in 1983. She was an advanced experimental technician in the Drugs Control of PAP, Beijing, China. Her research interests include neurology, neurography, and brain-computer interface.

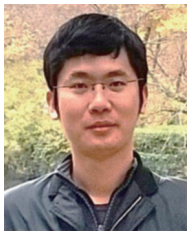

Wenchang Zhang received the BS degree from Shandong University of Technology, China, in 2004 and the MS degree from Academy of Military Medical Science, Beijing, China, in 2008. Currently, he is a PhD candidate in Department of Computer Sciences and Technology of Tsinghua University. Also, he is a research assistant at Academy of Military Science. His research interests include artificial intelligence, robotics, and brain-computer interface.

Fuchun Sun received the PhD degree in computer science from Tsinghua University in 1997. He is a full professor with the Department of Computer Science and Technology, Tsinghua University, China. His current research interest includes robotic perception and cognition. He was a recipient of the National Science Fund for Distinguished Young Scholars. He serves as an associate editor of a series of international journals including *IEEE Transactions on Systems, Man and Cybernetics: Systems*, *IEEE Transactions on Fuzzy Systems, Mechatronics*, and *Robotics and Autonomous Systems*. He is a fellow of the IEEE.

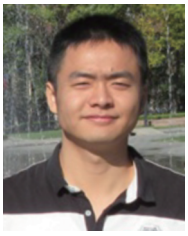

Hang Wu received the BS degree from Tianjin University, China, in 2012 and the PhD degree in biomedical engineering from Academy of Military Medical Science, Beijing, China, in 2017. Currently, he is a research assistant at Academy of Military Science. His main interests are robot vision and graphics processing, including visual terrain classification, remotely sensed image analysis, and pattern recognition.